Steel and Composite Structures, *Vol. 16, No. 4* (*2014*) *437-454*
DOI: http://dx.doi.org/10.12989/scs.2014.16.4.437

Influence of spacers on ultimate strength of intermediate length thin walled columns

M. Anbarasu * and S. Sukumar

Department of Civil Engineering, *Government College of Engineering*, *Salem – 636 011*, *Tamilnadu*, *India*

(*Received February 04*, *2013*, *Revised December 12*, *2013*, *Accepted December 17*, *2013*)

Abstract. The influence of spacers on the behaviour and ultimate capacity of intermediate length CFS open section columns under axial compression is investigated in this paper. The focus of the research lies in the cross- section predominantly, failed by distortional buckling. This paper made an attempt to either delay or eliminate the distortional buckling mode by the introduction of transverse elements referred herein as spacers. The cross-sections investigated have been selected by performing the elastic buckling analysis using CUFSM software. The test program considered three different columns having slenderness ratios of 35, 50 & 60. The test program consisted of 14 pure axial compression tests under hinged-hinged end condition. Models have been analysed using finite element simulations and the obtained results are compared with the experimental tests. The finite element package ABAQUS has been used to carry out non-linear analyses of the columns. The finite element model incorporates material, geometric non-linearities and initial geometric imperfection of the specimens. The work involves a wide parametric study in the column with spacers of varying depth and number of spacers. The results obtained from the study shows that the depth and number of spacers have significant influence on the behaviour and strength of the columns. Based on the nonlinear regression analysis the design equation is proposed for the selected section.

Keywords: cold-formed steel; column; distortional buckling; spacer; thin walled member

1. Introduction

In recent times, light gauge cold-formed steel sections have been used extensively in residential, industrial and commercial buildings as the primary load bearing structural components. This is because cold-formed steel sections have a very high strength to weight ratio compared with thicker hot-rolled steel sections, and their manufacturing process is simple and cost-effective. However, the structural behaviour of these thin-walled steel structures are characterized by a range of buckling modes such as local buckling, distortional buckling or flexural torsional buckling. These buckling problems generally lead to severe reduction and complicated calculations of their member strengths. Local modes and global modes (i.e. flexural and flexural-torsional buckling) are largely covered in the main design codes by means of effective widths of the plate elements and by column design equations for global buckling. Interaction of local and global modes is also

*Corresponding author, Assistant Professor, E-mail: gceanbu@gmail.com

http://www.techno-press.org/?journal=scs&subpage=8 ISSN: 1229-9367 (Print), 1598-6233 (Online)

considered in these codes. Distortional buckling plays an important role in the use of open cold formed steel columns. Distortional buckling occurs at intermediate length between the lengths where local and overall buckling occurs. Therefore it is important to eliminate or delay these buckling problems and simplify the strength calculations of cold-formed steel members.

A brief review of literature on the ultimate strength and buckling modes of cold-formed steel columns are presented here. Takahashi and Mizuno (1978) was the first to publish a paper describing distortion of the thin walled open section. Hancock (1985) presented a detailed study of a range of buckling modes (Local, distortional, and flexural-torsional) in a lipped channel section. Lau and Hancock (1990) provided simple analytical expressions to allow the distortional buckling stress to be calculated explicitly for any geometry of cross-section of thin-walled lipped-channel section columns. Kwon and Hancock (1992) studied simple lipped channels and lipped channels with intermediate stiffener under fixed boundary conditions. They choose section geometry and yield strength of steel to ensure that a substantial post-buckling strength reserve occurs in a distortional mode for the test section. Davies and Jiang (1998) used the Generalized Beam Theory to analyse the individual buckling modes either separately or in selected combinations.

The Distortional buckling strength of a few innovative and complex geometrical sections has been studied by Narayanan and Mahendran (2003). For intermediate length pallet rack columns, the distortional strength was studied by providing spacers to connect the flanges of upright sections by Talikoti and Bajoria (2005). The partly closed thin walled steel columns were studied by Veljkovic and Johanson (2008). Kwon *et al*. (2009) studied the buckling interaction of the channel columns. Anil Kumar and Kalyanaraman (2010) studied the evaluation of direct strength method for CFS Compression members without stiffeners. Shi *et al*. (2011) conducted tests and finite element analysis on the local buckling of 420 MPa steel equal angle columns under axial compression. Theofanous and Gardner (2011) studied the effect of element interaction and material nonlinearity on the ultimate capacity of stainless steel cross-sections. Anbarasu and Sukumar (2013a) studied the connectors interaction on the behaviour and ultimate strength of stiffened channel columns. Anbarasu and Sukumar (2013b) reported the effect of stiffener ties in the intermediate length cold formed steel (CFS) columns.

In conclusion, the existing research results show that the influence of spacers on the buckling behaviour and ultimate capacity of the axially loaded columns is less pronounced. So the distortional buckling strength of the intermediate columns under axial compression may be enhanced. However, sufficient research on the distortional buckling behaviour of complex stiffener members with spacers under axial compression is still in its infancy, which makes it necessary to perform a systematic study with both experimental and numerical investigations.

The main objective of this work is to examine the buckling behaviour and strength of intermediate length pin-ended column with spacers for which there are no design rules currently available. Spacers are the transverse elements of CFS sheet used to connect the lips of the sections using self-drilling screw. For this work, three types of channel shaped sections with complex stiffeners is considered. Totally 14 columns have been tested under pinned end condition. A numerical model is developed to trace the load deformation behaviour obtained from the experiments. Since, the cross sections are very thin and prone to buckling, shell element is used for FE modelling. Large deformation formulation, as well as, Elasto-plastic material response has been incorporated in the model. The finite element model is validated by the test results. In the present research, the finite element parametric study is carried out to investigate the effect of spacers by varying the depth and number of spacers on the ultimate capacity of the intermediate length columns.

2. Experimental investigation

2.1 Test specimens

The test program considered three different lipped channel cold formed shapes. For easy identification, the sections under consideration are referred as Type I, II and III, respectively. A total of 14 columns have been tested. Five column specimens including one fully opened and others with spacers from 1 to 4 have been tested to failure under axial compression for Type – I and Type – II columns. For Type – III columns, four column specimens including one fully opened and others with spacers from 1 to 3 have been tested. These sections are analyzed using CUFSM to find the most suitable geometry and length of the specimens. The length of specimen is selected as a multiple of buckling half wave lengths from CUFSM analyses. The dimensions of the cross sections are finalized keeping the plate slenderness ratio (Overall width of compression flange/thickness (b/t) ratio should not greater than 60) within limits to eliminate local buckling.

The ends of the columns are considered as pinned. The load factor versus half wave length plot is obtained by CUFSM software as shown in Fig. 1 for Type – III column. The two distinct minima in the plot represent the local buckling and distortional buckling. The local buckling mode of the Type – III column has a minimum of around 60mm in half wave length and the distortional mode has a minimum at 1067 mm in half wave length. The buckling plots for Type – I and Type – II columns are also obtained from CUFSM. From that the intermediate length is chosen to investigate distortional buckling for all the three types of columns as 1200 mm to eliminate global buckling effects. The nominal dimensions in mm and the geometry of the selected sections are shown in Fig. 2.

The specimens are fabricated by press braking operation. Spacers are the transverse elements made up of the same material of which is used for specimen is cut into required shape and connect the lips of the section using self-drilling screw. The self-drilling screws have the ability to drill their own hole and form, or tap their own internal threads without deforming their own thread. One screw of 6mm in diameter is used at each interconnection. Overall section dimensions were

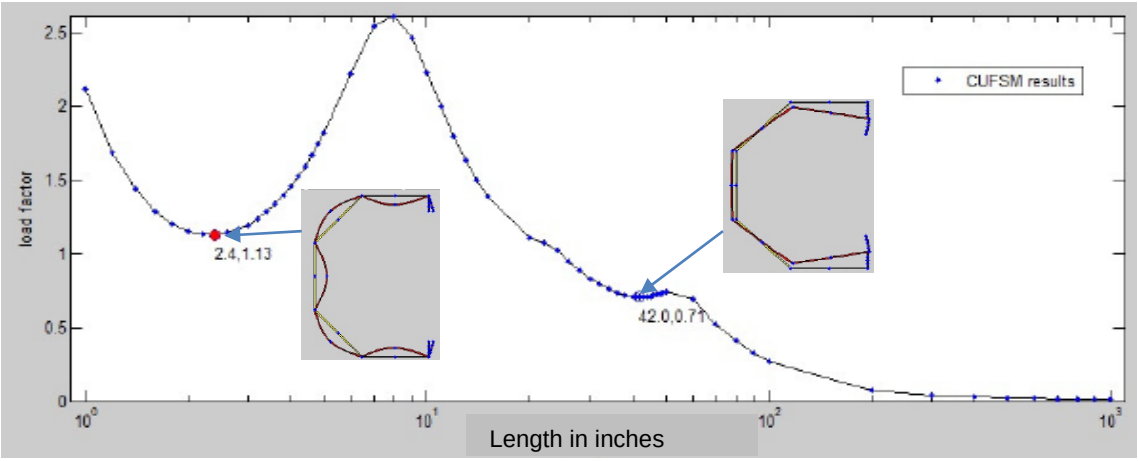

Fig. 1 Buckling plot of a selected section

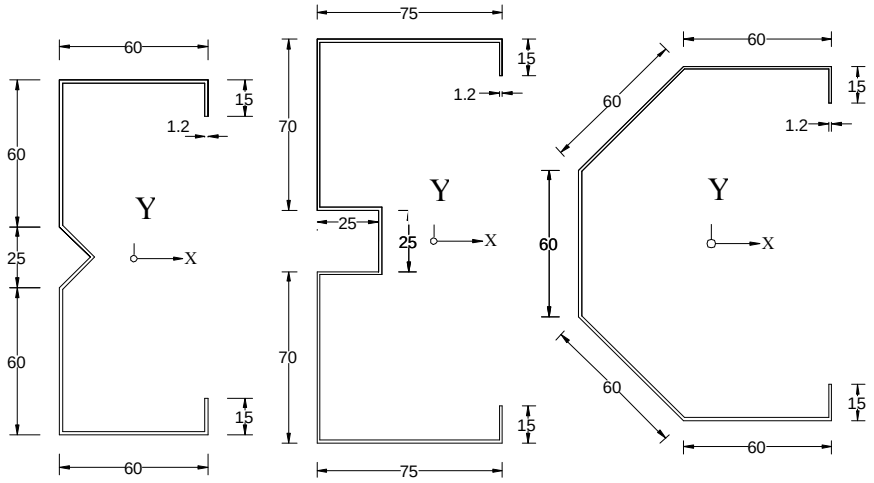

(a) Type – I (b) Type – II (c) Type – III

Fig. 2 Geometry and dimensions of the columns

Table 1 Measured cross-section dimensions of test specimens

Specimen Type	Average dimension of the specimens						
	A	B	C	D	E	t	L
Type – I	15.1	59.5	58.6	59.6	–	1.2	1200
Type – II	15.1	73.9	68.8	25.1	26.4	1.2	1201
Type – III	15.0	59.9	59.2	18.2	–	1.2	1202

measured for each test specimen, from which centreline dimensions of specimen cross-section were calculated. The measured dimensions were used for finite element modelling. Table 1 presents the values of the measured dimensions of test specimens. The press-braked specimens made for this research have sharp corners, and the corner radius was negligibly small.

2.2 Labeling

The naming convention for the test specimens is as below

$$\begin{Bmatrix} T1 \\ T2 \\ T3 \end{Bmatrix} - \begin{Bmatrix} S0 \\ S1 \\ S2 \\ S3 \\ S4 \\ S5 \end{Bmatrix} - \begin{Bmatrix} - \\ d20 \\ d30 \\ d40 \\ d50 \end{Bmatrix}$$

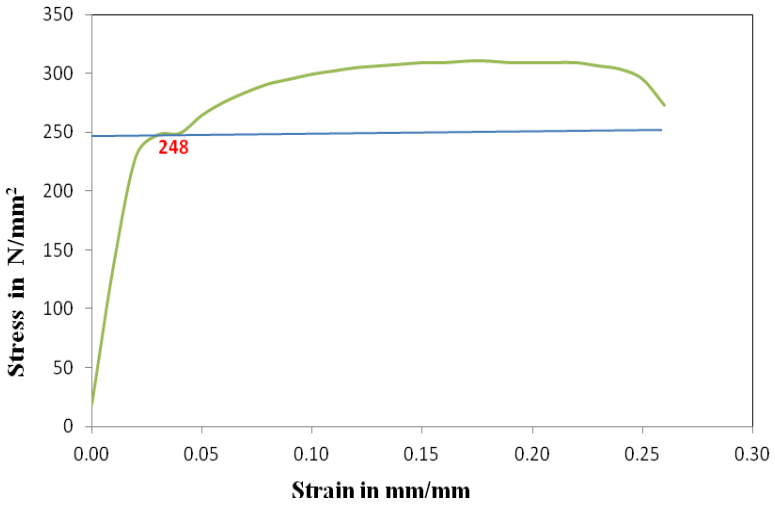

Fig. 3 Stress-strain curve of the coupon material

1st term:	Type of column:	*T*1 for type of column as 1
2nd term:	Number of spacers:	0, 1, 2, 3, 4 & 5.
3rd term:	Depth of spacer:	(blank) for open sections, *d*20 for depth of spacer = 20 mm

2.3 Tension coupon tests

The tensile coupon tests are carried out in accordance with IS 1608-2005 (Part-1). The stress-strain curves obtained from the coupon test is shown in Fig. 3. The material properties determined from coupon tests are also summarised below

Yield Stress (σ_y) =248MPa
Ultimate Stress (σ_u) = 310 MPa
Young's Modulus (E) = 2×10^5 MPa
Reduced Tangent Modulus (E_t) = 2000 MPa
Poisson's Ratio (ν) = 0.3
% of elongation = 27%

2.4 Test setup

The compression tests were carried out using the 400 kN capacity loading frame. The specimens had a 15 mm thick rectangular steel plate welded to each end. The specimens were mounted between the platens and its verticality was checked. All specimens were tested in pure axial compression with pinned end conditions. At either end between the platens and the end plates of the specimen rubber gaskets were placed to facilitate the pinned end condition at either supports Sukumar *et al*. (2003), Anbarasu and Sukumar (2013b).

A force control method was used to apply a uniformly distributed compression load gradually. Three LVDTs (Linear Variable Displacement Transducers) were used to measure the deformations of specimens during testing. The centroid axis of the end plates and the specimen cross section were kept the same to simulate a uniformly distributed load for pin-end conditions. The test configuration is shown in Fig. 4. The schematic diagram of the test setup is shown in Fig. 4(a) and

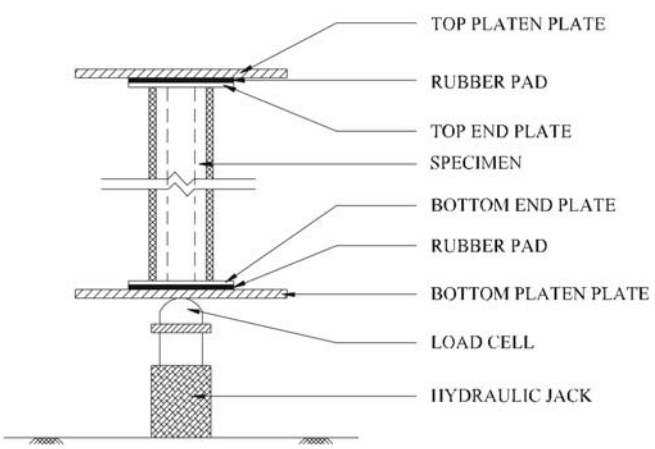

(a) Schematic diagram of test setup

(b) Test setup

Fig. 4 Test configuration

(a) (b)

(c)

Fig. 5 (a) Type – I tested specimens; (b) Type – II tested specimens; and (c) Type – III tested specimens

test set up in Fig. 4(b). The lateral and axial deformations of the column were recorded for every increment of load. The ultimate load at which the deflection increased without increase of load was also recorded.

2.5 Test results and discussion

The test buckling and test ultimate loads of the sections are summarized in Table 2. The final failure shape of the Type – I and Type – II open columns tested were mainly in the distortional mode which interacts with the local buckling mode as shown in Figs. 5(a) and (b). The spacers added Type – I and Type – II sections are failed by combined local (L), distortional (D) and minor axis flexural buckling (F) buckling mode. The interference of minor axis flexural buckling in the spacers added Type – I and Type – II sections made the ultimate loads increased only marginally.

But for the Type – III open section failure mode changes from combined distortional mode (D) and flexural torsional buckling (FT) to the interference of combined local (L), distortional (D) and flexural buckling (F) buckling mode due to the provision of spacers. The provision of spacers improves the torsional rigidity in the Type – III section alone. The deformed shapes of Type – III sections are shown in Fig. 5(c).

The ultimate stress σ_u of all the specimens, which is obtained by dividing the ultimate load P_u by the section area A, and the comparison with the measured yield strength σ_y are shown in Table 2. The addition of spacers in Type – I and Type – II sections not have much influence on the capacity but in Type – III sections have significant influence on the capacity. Therefore, this study focused on the parametric studies on Type – III section alone. The load vs axial shortening curves for tested specimens are shown in Fig. 6.

Table 2 Test results

Specimen ID	Experimental load, kN	Failure mode	Ultimate stress, σ_u N/mm^2	σ_u / σ_y
T1-S0	56.40	L + D	160.46	0.642
T1-S1-d20	58.40	L + D	162.75	0.651
T1-S2-d20	57.20	L + D	163.90	0.656
T1-S3-d20	58.40	L + D	167.34	0.669
T1-S4-d20	58.20	L + D	166.76	0.667
T2-S0	68.00	L + D	150.44	0.602
T2-S1-d20	70.00	L + D	154.87	0.619
T2-S2-d20	71.00	L + D	157.08	0.628
T2-S3-d20	71.20	L + D	157.52	0.630
T2-S4-d20	72.20	L + D	159.73	0.639
T3-S0	56.20	D + FT	149.87	0.599
T3-S1-d20	58.40	L + D + F	155.73	0.623
T3-S2-d20	64.20	L + D + F	171.20	0.685
T3-S3-d20	65.40	L + D + F	174.40	0.703

Note: L = Local buckling; D = Distortional buckling; F = Flexural buckling; and FT = Flexural Torsional buckling.

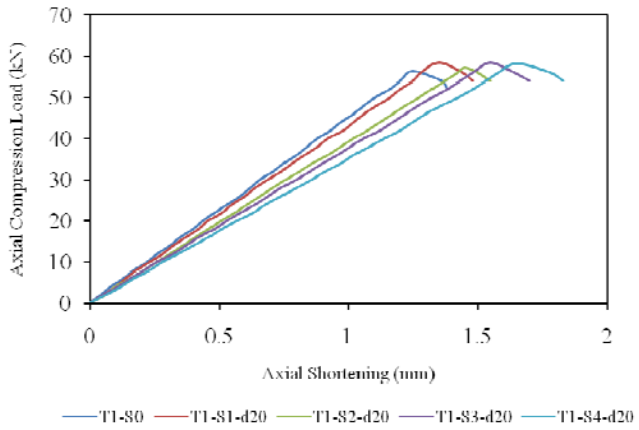

(a) For T1 Series

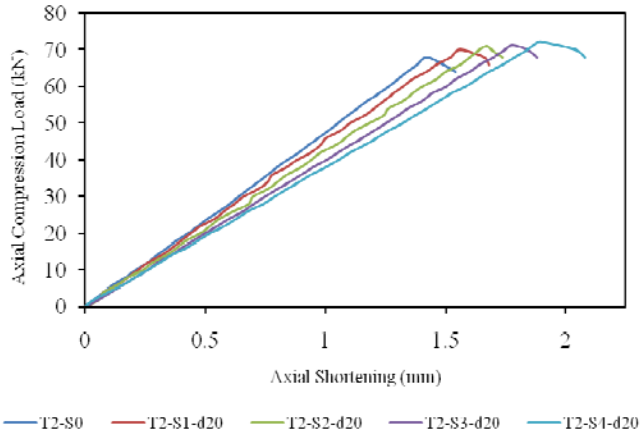

(b) For T2 Series

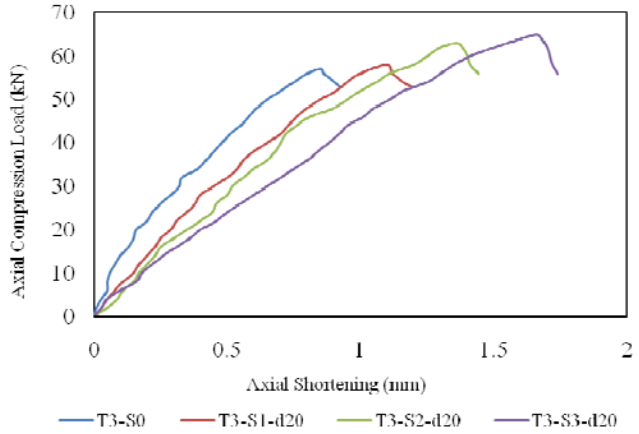

(c) For T3 Series

Fig. 6 Load Vs axial shortening curves for tested specimens

3. Numerical analysis

Numerical models were created using the general purpose finite element package ABAQUS are validated on the basis of test results. The models were based on the centre line dimensions of the cross-sections. The residual stresses and the rounded corners of the sections were not included in the model. The effect of residual stresses on the ultimate load is considered to be negligible as recommended by Schafer and Peköz (1998). The specimens were modelled using S4R5 shell elements. This element is only suitable for thin elements with small strains using the thin shell theory (also known as the Kirchhoff Love or Kirchhoff Shell Theory), however, large displacement and / or rotation is allowed. Convergence studies have been carried out on the column in order to determine the suitable mesh size for the finite element analysis.

The strain hardening of the corners due to cold forming is neglected. The boundary condition for both ends of the model is assigned to be an ideal pin end. At the bottom end, three translational degrees of freedom are restrained as well as the rotation about the longitudinal axis. The top end is restrained at the same as that of the unloaded end except for the translation in the longitudinal direction. The boundary conditions introduced to the centroid node and they were distributed to the other nodes through the MPC as shown in Fig. 7.

The screws have been modelled using Tie type MPC, which significantly simplifies the modelling of screws to connect the lips with spacer. This simplified representation of screws may neglect the effect of screw failures observed in the tests. The axial compression load was defined as a concentrated nodal force at the top. It was then distributed to the ends of the specimen through the MPC. Each node on the edge of the sections is considered a dependent node. These dependent nodes were then connected to the independent node which was created at the geometric centroid of the sections. They were connected by using rigid beams and hence they were controlled by the independent node. The displacement control loading method was used in the finite element analysis.

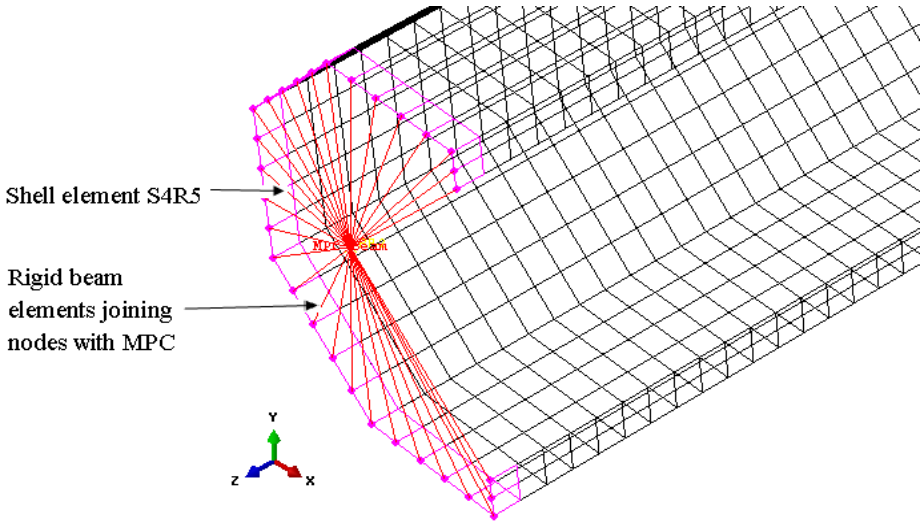

Fig. 7 Column ends modelled using MPC

Table 3 Comparison of results

Specimen ID	Test load, P_{test} kN	ABAQUS load, P_{FEA} kN	P_{test} / P_{FEA}
T1-S0	56.40	58.6	0.962
T1-S1-d20	58.40	61.20	0.954
T1-S2-d20	57.20	60.82	0.940
T1-S3-d20	58.40	61.44	0.951
T1-S4-d20	58.20	61.24	0.950
T2-S0	68.00	71.62	0.949
T2-S1-d20	70.00	74.32	0.955
T2-S2-d20	71.00	74.84	0.962
T2-S3-d20	71.20	75.43	0.957
T2-S4-d20	72.20	76.24	0.948
T3-S0	56.20	59.5	0.948
T3-S1-d20	58.40	61.95	0.943
T3-S2-d20	64.20	67.10	0.957
T3-S3-d20	65.40	68.25	0.984
Mean			0.952
Standard Deviation			0.007

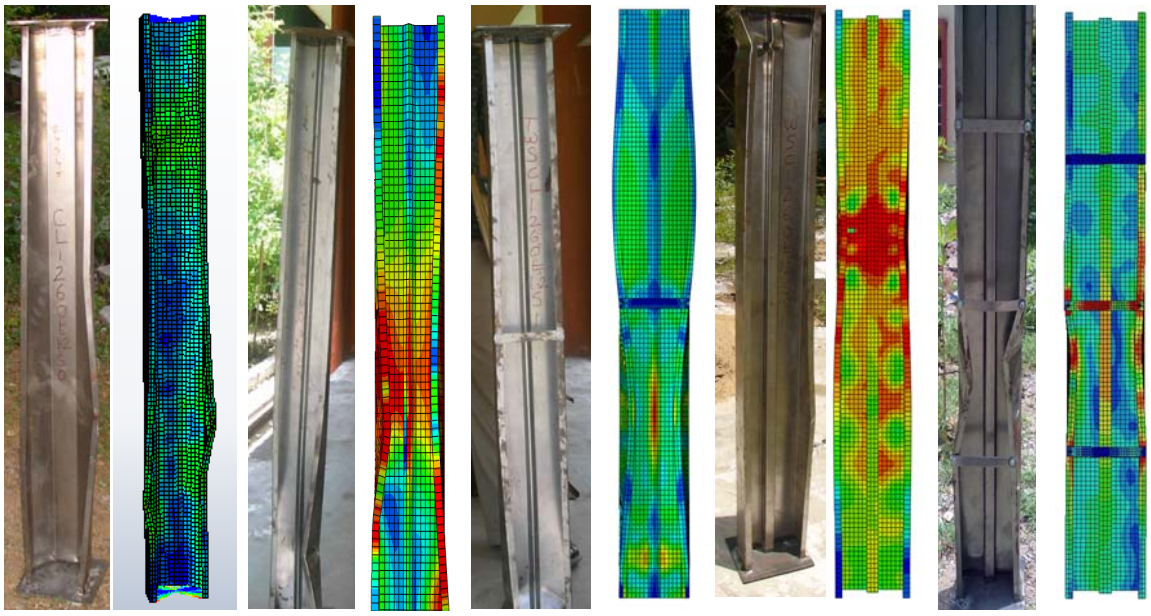

(a) For T3 - S0 (b) For T1 - S0 (c) For T1-S1-d20 (d) For T2 - S0 (e) For T2-S3-d20

Fig. 8 Comparison of experimental and FEA deformed shapes

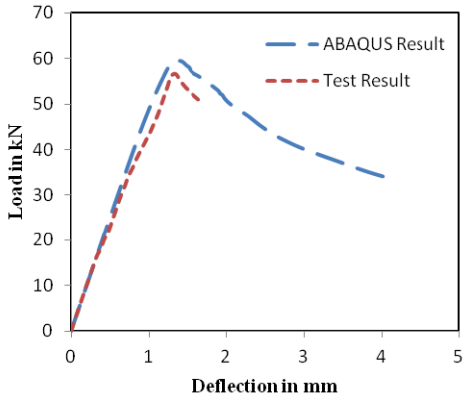

(a) For T3 - S0

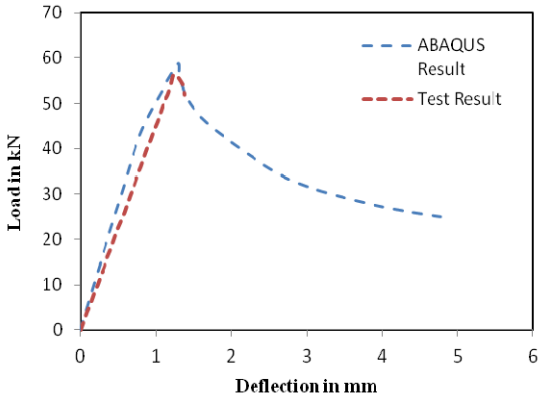

(b) For T1 - S0

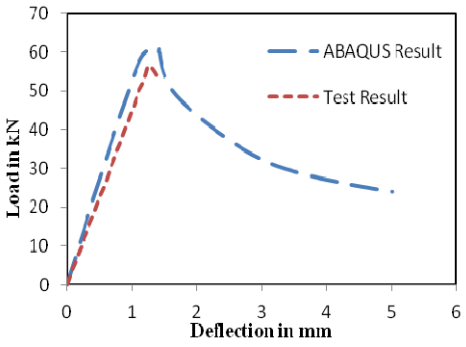

(c) For T1-S1-d20

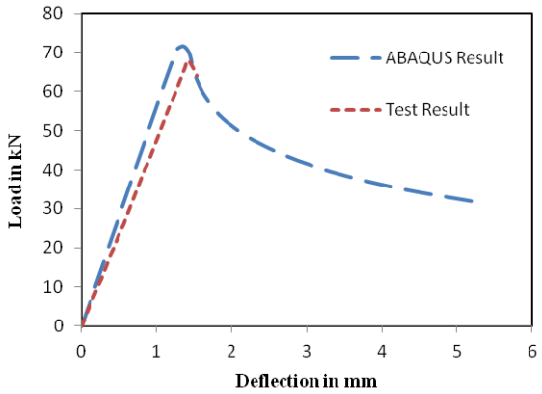

(d) For T2 - S0

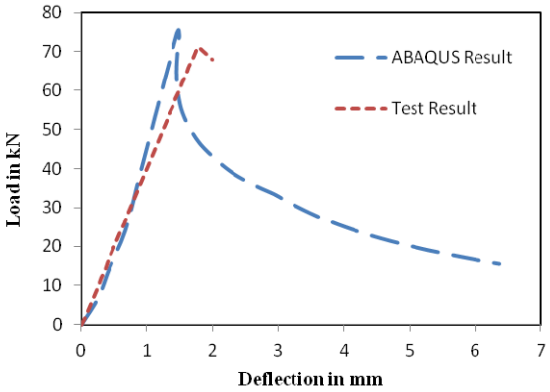

(e) For T2-S3-d20

Fig. 9 Comparison of test and FE analysis load vs. axial shortening curves

The material nonlinearity was included in the FEM by specifying the true values of stresses and strains. The engineering stresses and strains obtained from the tensile coupon tests were used to calculate the true stresses and strains. The plasticity of the material was simulated by a mathematical model, known as the incremental plasticity model, in which the true stresses and true plastic strains were calculated in accordance with ABAQUS. A non linear analysis was performed considering both geometric and material non linearities.

The load carrying capacity is mainly affected by geometric imperfections which arise from manufacturing, transportation and also from fabrication. This imperfection is simulated using buckling analysis of the specimen. Since, precise data on the distribution of geometric imperfection is not available, scaled value of linear buckling mode shape is used to create an initial geometric imperfection for the nonlinear buckling analysis. The degree of imperfection is assumed as the maximum amplitude of the buckling mode shape and considered as a percentage of the structure thickness. Two mode shapes namely local buckling and distortional buckling to incorporate imperfections are obtained by conducting eigen value analysis. Local buckling imperfection of 0.25 times the thickness and distortional buckling imperfection amplitude of 1 times thickness are used for validating the experimental specimens. The maximum value of distortional imperfection is taken equal to the plate thickness as recommended by Schafer and Peköz (1998), since kwon and Hancock (1992) found that the overall imperfections had little effect on the buckling of the columns of intermediate length therefore it was not included in this study.

4. Verification of finite element model

The results from the finite element analysis are compared with the failure modes, load-displacement curve, and ultimate capacity obtained from the tests. A comparison is carried out between the test results and the results of the finite element model to verify the accuracy of the finite element package. The test (P_{test}) and finite element analysis (P_{FEA}) results are compared in Table 3 which shows reasonable agreement.

The mean and standard deviation of the Test to FEA ultimate loads are 0.952 and 0.007 respectively. As an example, the load deflection curve obtained in FEA is compared with the test results for some of the sections are in Fig. 9 and it closely matches with the experimental results.

For most of the specimens, the ABAQUS results are slightly higher than the test results. The differences including variability in the ABAQUS model are more likely due to assumed imperfections, residual stress and the rounded corners of the sections are ignored.

Fig. 8 shows the comparison of buckled shape of tested specimens with the deformed shape of the specimens predicted by Finite element Analysis. The deformed shape obtained from the FEA has a reasonable agreement with the experimental buckling mode. Similar results have been obtained from other specimens also. Thus, the proposed finite element models are able to analyze the strength and buckling behaviour of columns under axial compression are readily applicable for further parametric studies.

5. Parametric study

The numerical analysis has been continued by conducting a parametric study on the influence of the depth and number of spacers on the ultimate strength of the Type – III columns under axial

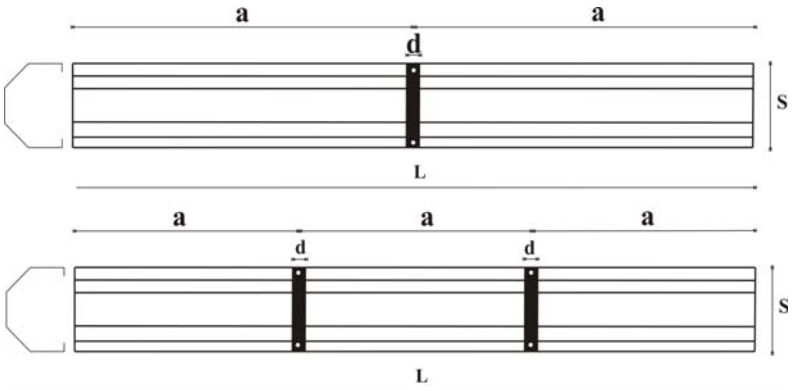

Fig. 10 Geometry of the columns

compression. The specimens were then analysed by considering the same boundary conditions as used in the experimental model. The initial geometric imperfections were included based on Schafer and Peköz (1998). The parameters which have direct influence on the response of the column are illustrated in Fig. 10.

- The term λ_s/λ which is defined as the ratio of the spacer plate slenderness to column slenderness

$$\lambda_S = \frac{d}{t} \times \sqrt{\frac{f_y}{E}}$$

Where, λ_s = Slenderness ratio of the spacer plate
λ = Slenderness ratio of the column
d = depth of spacer plate
t = thickness of spacer plate

- The term 'a/L' which is defined as the ratio of the center to center distance (a) between spacers-to-the overall length (L) of the Column
- The term 'd/S' which is defined as the ratio of the depth of the spacer plate-to-the breadth of the spacer plate

The parametric study included a total of 20 analysis cases. The two main parameters that were varied during the analysis are

- "d" the depth of the spacer plate, varied as 20 mm, 30 mm, 40 mm and 50 mm
- Number of spacers, varies from 1 to 5.

The width of the spacer and the slenderness ratio of the Type – III column is 240 mm and 35 respectively. Four groups of sections are formulated based on the 'd/S' ratio are 0.208, 0.312, & 0.417. Since the number of spacers varies from 1 to 5, the 'a/L' ratio varies from 0.50, 0.33, 0.25, 0.20 & 0.167. The λ_s/λ ratio varies from 0.017 to 0.208.

6. Numerical results

The normalized ratio of the ultimate-to-the yield stress of the column was influenced by various parameters and is graphically represented in the following subsections.

The plot for σ_u/σ_y versus a/L (Fig. 11) indicates that the relationship between the normalized ratio of the centre to centre length between spacers to the overall length of the Column (a/L), and the normalized ratio of the ultimate stress to the yield stress of the column (σ_u/σ_y) for different values of (d/S). Obviously, the centre to centre length between spacers has a significant effect on the strength of columns. Enhanced column strength values were obtained upon decreasing the spacers spacing (a). Increasing the number of spacers from 1 to 5 improved the ultimate strength of the columns. As the spacing of spacers (a) increases, the corresponding ultimate load decreases. The rate of increase in σ_u/σ_y is higher for lesser a/L ratios.

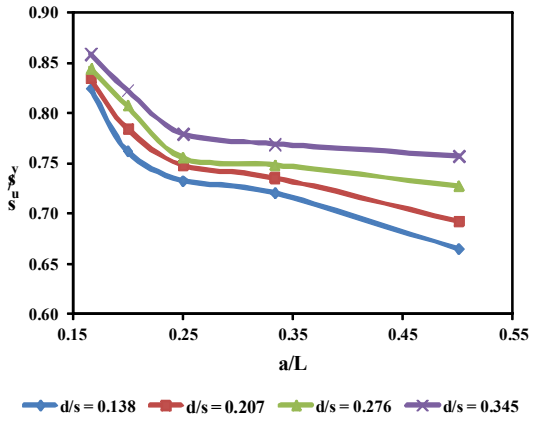

Fig. 11 σ_u/σ_y versus a/L curves

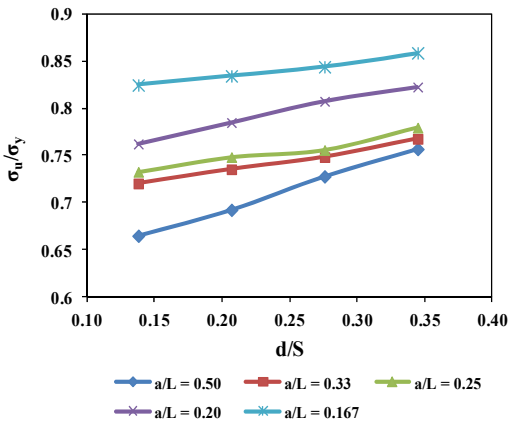

Fig. 12 σ_u/σ_y versus d/S curves

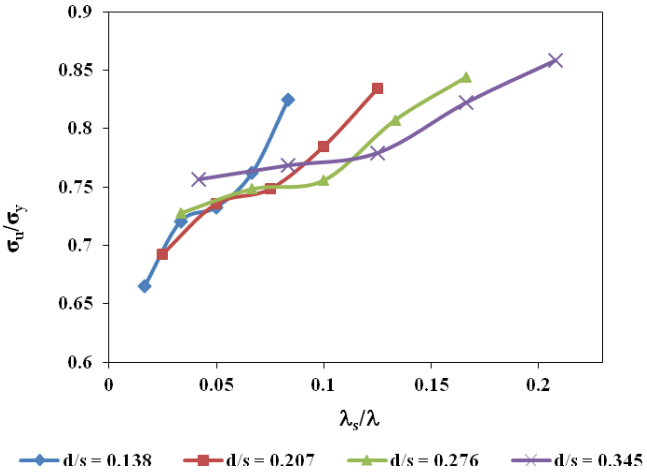

Fig. 13 σ_u/σ_y versus λ_s/λ curves

Table 4 Load carrying capacity of the type – III Column

Specimen ID	Load in kN	% increase
T3 – S0	59.50	---
T3 – S1 – d20	61.95	4.12
T3 – S2 – d20	67.10	12.77
T3 – S3 – d20	68.25	14.71
T3 – S4 – d20	71.00	19.33
T3 – S5 – d20	76.80	29.08
T3 – S1 – d30	64.51	8.42
T3 – S2 – d30	68.53	15.18
T3 – S3 – d30	69.70	17.14
T3 – S4 – d30	73.10	22.86
T3 – S5 – d30	77.70	30.59
T3 – S1 – d40	67.80	13.95
T3 – S2 – d40	69.72	17.18
T3 – S3 – d40	70.40	18.32
T3 – S4 – d40	75.20	26.39
T3 – S5 – d40	78.63	32.15
T3 – S1 – d50	70.51	18.50
T3 – S2 – d50	71.62	20.37
T3 – S3 – d50	72.10	21.18
T3 – S4 – d50	76.62	28.77
T3 – S5 – d50	79.97	34.40

The plot for σ_u/σ_y versus d/S (Fig. 12) demonstrates the influence of changing the depth of the spacer plate on the column strength for a slenderness ratio of 35. Apparently, as shown in Fig. 10 the column strength increases with the increase in depth of the spacer plate.

The plot for σ_u/σ_y versus λ_s/λ (Fig. 13) demonstrates the influence of the spacer plate slenderness ratio of the column strength for a slenderness ratio of 35. Apparently, as shown in Fig. 12 the column strength increases with the increase in plate slenderness ratio. The percentage increase in ultimate load of the column while varying the depth and number of spacers are shown in Table 4.

7. Regression analysis

An empirical design equation was developed for the ultimate strength of the Type –III column (P_u) as a function of the ratio of the slenderness of the spacer plate to column (λ_s/λ), the ratio of length (a/L) and ratio of depth to width of the spacer plate (d/S). Since it is based upon the results of the parametric study, it allows for all of the parameters varied in the parametric study. The plot for σ_u/σ_y versus λ_s/λ, a/L and d/S shown in Figs. 10, 11 and 12 indicates that variation is non-

linear.

A non-linear regression analysis is carried out using statistical analysis software SPSS to estimate the models with arbitrary relationship between the dependent variable (σ_u/σ_y) and a set of independent variables (λ_s/λ, a/L and d/S). This is accomplished using iterative estimation algorithms. For each iteration, parameter estimates and the residual sum of squares is obtained. For the assumed model, the sum of squares for regression, residual, uncorrected total and corrected total, parameter estimates, asymptotic standard errors, and asymptotic correlation matrix of parameter estimates are evaluated. The best fit for any assumed relationship between dependent and independent parameters can be ensured only if R-squared [1-(Residual sum of squares/ Corrected sum of squares)] value is more than 0.95. The following design equations for the Type – III column is developed using nonlinear regression analysis.

$$\frac{\sigma_u}{\sigma_y} = \left[-0.24 * \frac{\lambda_S}{\lambda}\right] + \left[12.54 * \frac{a}{L}\right] - \left[29.14 * \left(\frac{\lambda_S}{\lambda}\right)^{0.28} * \left(\frac{a}{L}\right)^{1.12}\right] + \left[0.93 * \left(\frac{\lambda_S}{\lambda}\right)^{-0.61} * \left(\frac{d}{s}\right)^{1.48}\right] + 0.74$$

It is found that for the above mentioned proposed design Eq. (1) the *R*-squared value (1-(Residual sum of squares/Corrected sum of squares)) is found to be 0.981 which is more than 0.95. Hence best fits the data obtained using nonlinear regression analysis.

8. Discussions

The results presented in this paper illustrate a number of important points in relation to the performance of behaviour and ultimate capacity of an intermediate length column with spacers. From the parametric study, it is ascertained that interaction between the parameters like the ratio of the slenderness of the spacer plate to column (λ_s/λ), the ratio of length (a/L) and ratio of depth to width of the spacer plate (d/S) influence the strength of the columns. With the addition of spacers in the columns, the failure mode shifted from combined flexural torsional buckling and distortional mode to the interference of combined flexural buckling and distortional buckling mode. From the ultimate loads of all the columns with a number of spacers 1, 2, 3, 4 and 5 it is inferred that the improvement in torsional rigidity increases the load carrying capacity. The percentage increase in the ultimate load of the column with different depth such as 20 mm, 30 mm, 40 mm and 50 mm spacers over fully opened section ranges from 4.12 to 34.40%.

9. Conclusions

This paper has described a detailed investigation into the structural behaviour of intermediate length cold-formed steel compression members with and without spacers under axial compression. Both experimental and finite element analyses were conducted to improve the knowledge and understanding of the behaviour of intermediate length cold-formed steel compression members subjected to axial compression, and hence this has led to safer structural design methods for columns with spacers. The cold-formed steel sections can be designed to fail by distortional buckling by choosing their geometry based on the buckling plots from the simple finite strip analysis programs such as CUFSM.

Finite element models of testing cold-formed steel compression members were developed using the advanced finite element tool ABAQUS. They are validated by comparing their results with the corresponding experimental results: ultimate loads, load vs axial shortening curves and deflected shapes. The validated finite element models are then used to undertake an extensive parametric study by varying the depth and number of spacers. The parametric study results are used to develop a design equation to predict the ultimate loads of light gauge cold-formed steel compression members with spacers subjected to axial compression. Based on the study, the following conclusions are drawn within the limit of the present investigation.

- Adding the spacers has a significant effect on improvement in ultimate load capacity on the intermediate length Type – III columns.
- For Type – III columns the ultimate load capacity increases with increase in depth and number of spacers.
- The addition of spacers improves the load carrying capacity of the Type – III column by enhancing the torsional rigidity of the section.
- The ultimate load capacity has little effect due to the addition of spacers in the Type – I and Type – II columns.
- It is also concluded from the study that all the section profiles in intermediate length may not have the improvement in the ultimate capacity of the columns by the addition of spacers.
- From this investigation it is observed that the use of spacers at the proper depth and spacing do help to increase not only ultimate load capacity but also change the mode of failure.
- The finite element modelling using ABAQUS software is sufficiently accurate in predicting the ultimate load capacity and behaviour of the columns. Therefore, the finite element analysis can be used with a high level of confidence in predicting the load capacity of axially loaded cold formed steel intermediate length columns with spacers.
- The proposed strength formula for the Type – III columns can reasonably predict the ultimate strength of intermediate length cold-formed steel columns with spacers.

This study shows that further research is needed in this area to have more experimental data to add the design codal provisions for the interaction of spacers in the ultimate load capacity of intermediate length cold-formed steel columns.

References

Anbarasu, M. and Sukumar, S. (2013a), "Effect of connectors interaction in behaviour and ultimate strength of intermediate length Cold Formed Steel (CFS) open columns", *Asian J. Civil Eng.*, **14**(2), 305-317.

Anbarasu, M. and Sukumar, S. (2013b), "Study on the effect of ties in the intermediate length cold formed steel (CFS) columns", *Struct. Eng. Mech., Int. J.*, **46**(3), 323-335.

Anil Kumar, M.V. and Kalyanaraman, V (2010), "Evaluation of direct strength method for CFS compression members without stiffeners", *J. Struct. Eng.*, **136**(7), 879-885.

AS/NZS 4600:2005 (2005), "Australian / New Zealand Standard – Cold Formed Steel Structures".

Davises, J.M. and Jiang, C. (1998), "Design for distortional buckling", *J. Construct. Steel Res.*, **46**, 174-175.

Hancock, G.J. (1985), "Distortional buckling of steel storage rack column", *J. Struct. Eng., ASCE*, **111**(12), 2770-2783.

Kwon, Y.B. and Hancock, G.J. (1992), "Tests of cold formed channel with local and distortional buckling", *J. Struct. Eng. ASCE*, **118**(7), 1786-1803.

Kwon, Y.B., Kim, B.S. and Hancock, G.J. (2009), "Compression tests of high strength cold-formed steel

channels with buckling interaction", *J. Construct. Steel Res.*, **65**(2), 278-289.
Lau, S.C.W. and Hancock G.J. (1990), "Inelastic buckling of channel columns in the distortional mode", *Thin-Wall. Struct.*, **10**(1), 59-84
Narayanan, S. and Mahendran, M. (2003), "Ultimate capacity of innovative cold-formed steel columns", *J. Construct. Steel Res.*, **59**(4), 489-508.
North American Specification (NAS) (2007), "Specification for the design of cold–formed steel members", *North American Cold-formed Steel Specification*, *American Iron and Steel Institute*, Washington, D.C., USA.
Schafer, B.W. and Peköz, T. (1998), "Computational modelling of cold-formed steel: characterizing geometric imperfections and residual stresses", *J. Construct. Steel Res.*, **47**(3)**,** 193-210.
Shi, G., Liu, Z., Ban, H.Y., Zhang, Y., Shi, Y.J. and Wang, Y.Q. (2011), "Tests and finite element analysis on the local buckling of 420 MPa steel equal angle columns under axial compression", *Steel Compos. Struct.*, *Int. J.*, **12**(1), 31-51.
Sukumar, S. Parameswaran, P. and Jayagopal, L.S. (2003), "Behaviour of built-up open cross-sections under axial load", *J. Struct. Eng.*, *SERC*, *India*, **30**(2) 89-94.
Takahashi, K. and Mizuno, M. (1978), "Distortion of thin-walled open section members", *Bulletin Jpn. Soc. Mech. Eng.*, **21**(160), 1448-1458.
Talikoti, R.S. and Bajoria, K.M. (2005), "New approach to improving distortional strength of intermediate length thin-walled open section columns", *Electron. J. Struct. Eng.*, **5**, 69-79.
Theofanous, M. and Gardner L., (2011) "Effect of element interaction and material nonlinearity on the ultimate capacity of stainless steel cross-sections", *Steel Compos. Struct.*, *Int. J.*, **12**(1), 73-92.
Veljkovic, M. and Johansson, B. (2008), "Thin-walled steel columns with partially closed cross-section: Tests and computer simulations", *J. Construct. Steel Res.*, **64**(7-8), 816-821.

CC